Thin Solid Films xxx (2012) xxx–xxx

Contents lists available at SciVerse ScienceDirect

Thin Solid Films

journal homepage: www.elsevier.com/locate/tsf

Structural and optical properties of Cu_2ZnSnS_4 thin film absorbers from ZnS and Cu_3SnS_4 nanoparticle precursors

Xianzhong Lin [a,*], Jaison Kavalakkatt [a,b], Kai Kornhuber [a], Sergiu Levcenko [a], Martha Ch. Lux-Steiner [a,b], Ahmed Ennaoui [a,*]

[a] Helmholtz-Zentrum Berlin für Materialien und Energie GmbH, Hahn-Meitner-Platz 1, D-14109 Berlin, Germany
[b] Freie Universität Berlin, Berlin, Germany

ARTICLE INFO

Available online xxxx

Keywords:
Cu_2ZnSnS_4
CZTS
Optical properties
Raman spectroscopy
Photoluminescence

ABSTRACT

Cu_2ZnSnS_4 (CZTS) has been considered as an alternative absorber layer to Cu(In,Ga)Se_2 due to its earth abundant and environmentally friendly constituents, optimal direct band gap of 1.4–1.6 eV and high absorption coefficient in the visible range. In this work, we propose a solution-based chemical route for the preparation of CZTS thin film absorbers by spin coating of the precursor inks composed of Cu_3SnS_4 and ZnS NPs and annealing in Ar/H_2S atmosphere. X-ray diffraction and Raman spectroscopy were used to characterize the structural properties. The chemical composition was determined by energy dispersive X-ray spectroscopy. Optical properties of the CZTS thin film absorbers were studied by transmission, reflection and photoluminescence spectroscopy.

1. Introduction

Cu_2ZnSnS_4 (CZTS) has been considered as an alternative absorber layer to Cu(In,Ga)Se_2 due to its earth abundant and environmentally friendly constituents, optimal direct band gap of 1.4–1.6 eV and high absorption coefficient ($>10^4$ cm^{-1}) in the visible range [1,2]. In recent years, great efforts have been focusing on the preparation of CZTS thin films and exploration of their potential application in thin film solar cells [2–10]. The preparation of CZTS thin films can be summarized as two methods, namely vacuum-based processes and non-vacuum solution-based processes [11]. More specifically, vacuum-based processes include sputtering and evaporation while non-vacuum based processes include electrodeposition, spray pyrolysis, and ink-based approaches [2–10,12]. The solution processes such as ink rolling and printing which allow the large scale deposition of thin films are considered as one of the low cost routes for fabrication of electronic devices. $Cu_2ZnSnSe_4$ and $Cu_2ZnSn(S, Se)_4$-based solar cells using a hydrazine-based solution process have already reached an energy conversion efficiency as high as 10.1% [3,4], demonstrating the effectiveness of the solution processes in CZTSe-based solar cells. In this contribution, we propose a solution-based chemical route for the preparation of CZTS thin film absorbers from Cu_3SnS_4 and ZnS nanoparticle precursors. The structural and optical properties have been studied by X-ray diffraction, Raman spectroscopy, transmission, reflection and photoluminescence spectroscopy.

2. Experimental details

2.1. Preparation of Cu_3SnS_4 and ZnS nanoparticle inks

ZnS NPs (NPs) were prepared according to the literature [13] with some modification. Briefly, stoichiometric zinc acetate dihydrate and sulfur were mixed together with oleylamine and heated to 240 °C to allow formation of ZnS NPs. Cu_3SnS_4 NPs were synthesized by one pot techniques based on the method reported on reference [14] where copper acetylacetonate, tin chloride, sulfur and oleylamine were mixed together in one vessel and heated to 250 °C to allow the reaction to take place. In this approach, oleylamine was used as both solvent and stabilizer. The inks were formed by mixing certain amount of ZnS and Cu_3SnS_4 NPs dispersed in hexanethiol.

2.2. Preparation of thin films

Thin films were deposited on different substrates (Mo/glass, 10 nm Sn on Mo/glass and 20 nm Sn on Mo/glass substrates) by spin coating using the precursor inks, followed by sequential heat treatment at 200 °C for 5 min in air to remove the solvent. After that, the resulting precursor thin films were annealed at 540 °C under Ar/H_2S (5%)-atmosphere for 60 min to allow the formation of CZTS absorber by the reaction of Cu_3SnS_4 and ZnS NP precursors. In order to study the optical transmission and reflection properties, corresponding samples on soda lime glass and tin layer coated soda lime glass were prepared. Note that, prior to the film coating, the glass and Mo/glass substrates were cleaned by subsequent ultrasonication in acetone, ethanol and distilled water, each for 15 min and dried under nitrogen stream.

* Corresponding authors.
E-mail addresses: lin.xianzhong@helmholtz-berlin.de (X. Lin), ennaoui@helmholtz-berlin.de (A. Ennaoui).

0040-6090/$ – see front matter © 2012 Elsevier B.V. All rights reserved.
http://dx.doi.org/10.1016/j.tsf.2012.10.034

2.3. Characterization

The structure of the films was studied by X-ray diffraction (XRD) and Raman spectroscopy. XRD were operated in the 2θ range from 10 to 90° on a Bruker D8-Advance X-ray diffractometer with CuKα radiation (λ = 1.5406 Å) using a step size of 0.02° and step time of 0.3 s. For the Raman measurement a Ti:Sapphire-ring-laser was used as an excitation. The wavelength of the laser is fully tenable from 690 nm to 1050 nm. To avoid laser heating the beam power was kept below 3.5 mW. Raman spectra were recorded with a Horiba T64000 triple monochromator system in backscattering configuration with a microscope and a motorized XY stage. The micro-Raman spectroscopy with a 100× objective was performed at room temperature with a wavelength of 747 nm. The chemical compositions were obtained by energy dispersive X-ray spectroscopy analysis (EDX) which was performed in a LEO GEMINI 1530 field-emission gun scanning electron microscope (SEM) with the operating voltage of 10 kV and a Thermo Noran X-ray silicon drift detector (acquisition and evaluation software Noran System Seven). The absorption was characterized through transmission and reflection measurements performed with a Lambda 950 UV–vis spectrometer. Photoluminescence (PL) was performed at room temperature using an excitation diode laser with a wavelength of 660 nm and a silicon CCD camera.

3. Results and discussion

3.1. Structural properties

Fig. 1 shows the XRD patterns of as-deposited and annealed samples on different substrates. Bragg peaks belonging to phases of $Cu_{2-x}S$ can be observed in the XRD patterns of as-deposited samples, which may be due to the decomposition of Cu_3SnS_4 precursors during the heat treatment process. However, these Bragg peaks disappear after annealing. The appearance of the Bragg peaks of (020), (101), (110), (103) and (202) which belong to kesterite CZTS (JCPDS data file no.: 26-0575(CZTS)) were observed in all three annealed samples, indicating the formation of kesterite phase of CZTS. Although two of the samples were prepared on molybdenum coated glass substrates with 10 and 20 nm tin layer on top we cannot find any Bragg peaks corresponding to Sn_xS_y after annealing at 540 °C. This suggests that the tin layer converted to CZTS by reaction with H_2S, ZnS and Cu_3SnS_4. In addition to the kesterite CZTS and Mo Bragg peaks, peaks ascribed to MoS_2 phase were also identified. Note that the relative intensity of MoS_2 Bragg peak is much more intensive in Mo coated with tin layer samples than in the bare Mo substrate sample. This phenomenon can be explained as the better penetration of H_2S through the tunnel created by the diffusion of tin underneath the nanoparticle layer during annealing process. It is known that the main XRD peaks among kesterite CZTS, ZnS and CTS are overlapping, as shown in Fig. 1. Therefore, although no noticeable peak ascribed to the other secondary phases can be observed except for the Mo and MoS_2 Bragg peaks we cannot conclude that both ZnS and CTS NPs precursors have reacted completely and transformed to CZTS.

In order to find out the existence of the secondary phases, Raman spectroscopy was performed. Fig. 2 shows the Raman spectra of annealed samples on different substrates. The strongest peak P1 in all three samples is located at 337–338 cm^{-1}, which is identified as the main vibrational A symmetry mode from kesterite CZTS [9–11,15,16]. The weaker peaks at about 264–266, 288, and 364–375 cm^{-1} were also found by fitting the spectra with Lorentzian curves, and can be attributed to kesterite CZTS [9–11,15,16]. Note that the peak at 364–375 cm^{-1} is split into two peaks, P3 and P4 centered at 364–368 and 374–377 cm^{-1}, respectively. This may be due to the use of excitation laser wavelength of 747 nm during the measurements, which is in agreement with the report by Fernandes et al. [10] who studied the effect of excitation laser wavelength on the Raman spectra of CZTS and found that the peak at 368 cm^{-1} separated into two peaks when using an excitation laser with a wavelength of 785 nm. Moreover, the Raman spectra in all three samples also show additional weaker broad peaks P6 in the region of 305–315 cm^{-1}. The possible contribution of the broad peaks could come from the phase of cubic Cu_2SnS_3, SnS_2 and Cu_3SnS_4 which are reported to have vibration modes at 303, 314 and 318 cm^{-1} respectively [17,18]. However, the presence of SnS_2 can be ruled out due to the absence of the Bragg peaks of SnS_2 in XRD patterns. The peak P7 located at 411–413 cm^{-1} indicates the presence of MoS_2, which further confirmed the XRD results [15].

3.2. Chemical composition

The chemical compositions of the as-deposited and annealed thin films on Mo substrates were studied using EDX measurements, as shown in Table 1. Due to the overlap between sulfur Kα peak and molybdenum Lα peak, EDX cannot resolve sulfur from molybdenum.

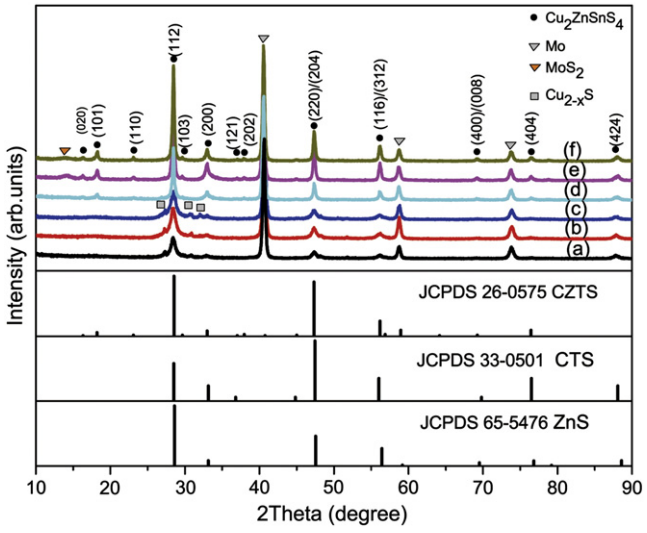

Fig. 1. X-ray diffraction patterns of: as-deposited precursor thin films prepared on (a) Mo/glass substrate, (b) Mo/glass substrate coated with 10 nm Sn layer, (c) Mo/glass substrate coated with 20 nm Sn layer and corresponding annealed samples: (d), (e), and (f). For reference, the XRD patterns of CZTS (JCPDS 26–0575), Cu_3SnS_4 (JCPDS 33–0501) and ZnS (65–5476) are shown below.

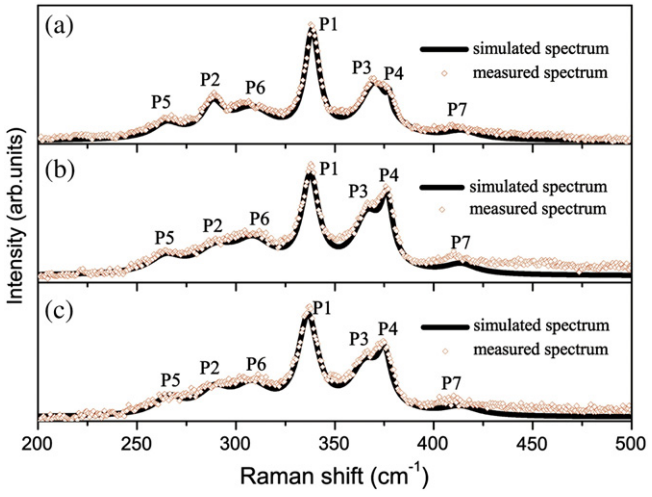

Fig. 2. Raman spectra of annealed CZTS thin films prepared on different substrates: (a) Mo/glass substrate, (b)Mo/glass substrate coated with 10 nm Sn layer, and (c) Mo/glass substrate coated with 20 nm Sn layer. Seven peaks were observed in all three samples (P1 (338 cm^{-1}), P2 (288 cm^{-1}), P3 (366 cm^{-1}), P4 (376 cm^{-1}), P5 (264 cm^{-1}), P6 (305–315 cm^{-1}) and P7 (412 cm^{-1})).

Please cite this article as: X. Lin, et al., Thin Solid Films (2012), http://dx.doi.org/10.1016/j.tsf.2012.10.034

Therefore, only the compositions of metal components are shown. As shown in Table 1 (a) the as-deposited samples are slightly Cu-rich and Sn-poor. Table 1 (b) shows the compositions of the corresponding annealed samples. It is found that the compositions of Cu and Sn decrease while the composition of Zn increases in all three annealed samples. The reduction of Cu and Sn is considered to be due to evaporation, since the structural analysis demonstrated that there are no $Cu_{2-x}S$ or SnS_x secondary phases in the annealed CZTS thin films. Note that, the ratio of Zn (33.4 at.%) in the Mo substrate sample after annealing is far from stoichiometry which may suggests the existence of ZnS secondary phase although there is no noticeable peak attributed to this phase in Raman spectrum.

3.3. Optical properties

The optical properties of the annealed CZTS thin films were studied by optical transmission, reflection and photoluminescence measurement at room temperature. The optical absorption coefficient (α) was determined from the measured transmittance (T) and reflectance (R) using the formula [19]

$$\alpha = \frac{1}{t}\ln\left[\frac{(1-R)^2}{T}\right] \quad (1)$$

where t is the thickness of the film. The absorption coefficient of the three samples is larger than 10^4 cm^{-1} in the visible region. The plot of $(\alpha h\nu)^2$ versus the photon energy ($h\nu$) for the annealed CZTS thin films prepared on three different substrates, namely glass substrate, 10 nm tin layer coated glass substrate and 20 nm tin layer coated glass substrate, is presented in Fig. 3. The optical band gap is obtained using the following equation [19]

$$(\alpha h\nu) = A\left(h\nu - E_g\right)^n \quad (2)$$

where α is the optical absorption coefficient, A is a constant, E_g is the optical band gap and $n = 1/2$ for direct transition. The optical band gap was obtained by extrapolating the linear region of the plot $(\alpha h\nu)^2$ versus photon energy ($h\nu$). Therefore the estimated optical band gaps of the CZTS thin films on glass, 10 nm tin coated glass and 20 nm tin coated glass substrates are 1.55, 1.50 and 1.48 eV respectively, which are in good agreement with the previously reported values of 1.4–1.6 eV [1,2,9,20]. When comparing the optical band gaps with compositions of the CZTS thin films we found that there is a decrease in optical band gap with increasing $Cu/(Zn+Sn)$ ratio. This is in accordance with previous reports [20,21] where the optical band gap shifted toward higher energies as the $Cu/(Zn+Sn)$ ratio of the CZTS thin film decreased. The optical band gap of semiconductor materials is determined by the valence band maximum and the conduction band minimum. The valence band maximum of CZTS is related to the antibonding of Cu 3d and S 3p [22,23]. Therefore, the shift of the band gap may be due to the increase of valence band maximum with increasing $Cu/(Zn+Sn)$ ratio.

Table 1
Chemical composition of metal compoments of: (a) as-deposited precursor thin films; (b) annealed CZTS thin films using EDX measurements.

Substrates	Cu (at.%)	Zn (at.%)	Sn (at.%)	Cu/(Zn + Sn)	Zn/Sn
(a) As-deposited					
Mo/glass	54	28	18	1.17	1.55
10 nm Sn/Mo/glass	52	26	22	1.08	1.18
20 nm Sn/Mo/glass	51	25	24		1.04
(b) After annealing					
Mo/glass	49	33	18	0.96	1.83
10 nm Sn/Mo/glass	50	30	20	1.00	1.50
20 nm Sn/Mo/glass	51	27	22	1.04	1.23

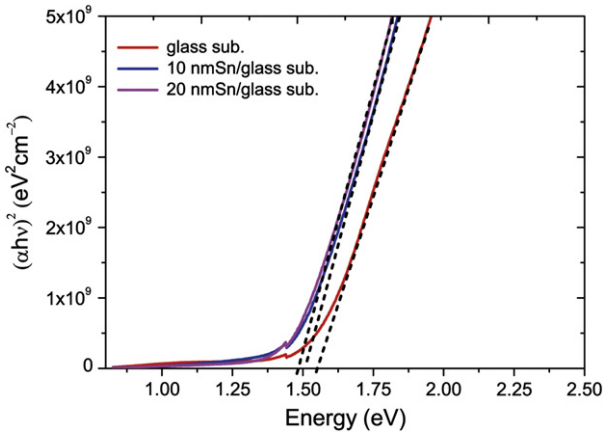

Fig. 3. Plot of $(\alpha h\nu)^2$ versus $h\nu$ for annealed CZTS thin films prepared on glass and tin layer coated glass substrates.

Fig. 4 compares the PL spectra of annealed samples deposited on different substrates. All three samples show broad PL band centered at about 1.35 eV, 1.30 eV and 1.28 eV, which are smaller than the corresponding optical band gaps. This observation points to the defect related type recombination in CZTS thin films. The absence of transitions from band to band in PL spectra may be attributed to the fact that defect type recombination is the dominant recombination channel in this material due to the large number of possible intrinsic defects in CZTS material [24]. It is interesting to note, that the peak positions suffer red shift as $Cu/(Zn+Sn)$ ratio of the CZTS thin films increased, which shows the same variation trend with the optical band gaps determined by transmission and reflection measurements. The found correlation between PL and absorbance results may be ascribed to the presence of the same defect, which has a state with an energy separation from one of the band edges which is only weakly composition dependent. The excitation power dependent low temperature measurements on the sample prepared on Mo substrate coated with 10 nm tin layer show that the peak positions exhibit a blue shift of about 5 meV per decade with increasing of the excitation power. This blue shift of the PL band peak positions reveals a donor-acceptor recombination process [25,26].

4. Conclusions

CZTS thin films have been prepared via spin coating using Cu_3SnS_4 and ZnS nanoparticle inks followed by annealing under Ar/H_2S

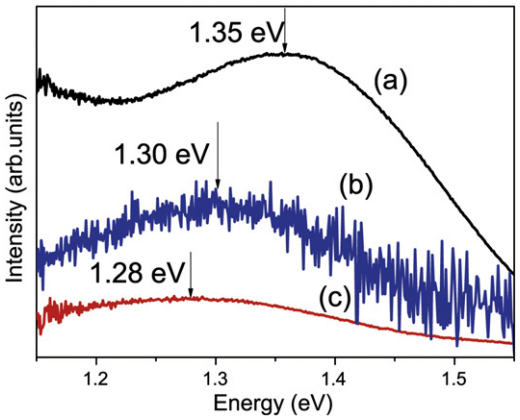

Fig. 4. PL spectra of annealed samples on (a) Mo/glass substrate, (b) Mo/glass substrate coated with 10 nm Sn layer and (c) Mo/glass substrate coated with 20 nm Sn layer measured at room temperature.

Please cite this article as: X. Lin, et al., Thin Solid Films (2012), http://dx.doi.org/10.1016/j.tsf.2012.10.034

atmosphere. The structural analysis reveals the formation of CZTS absorbers with a kesterite structure after annealing at 540 °C under Ar/H_2S atmosphere. Optical analysis indicates that the optical band gaps of the three samples are 1.55, 1.50 and 1.48 eV, which is ideal for solar energy conversion. The optical band gaps as well as the PL peak positions shifted toward higher energies as $Cu/(Zn+Sn)$ ratio of the CZTS thin films decreased.

Acknowledgments

This work was carried out as part of a program supported by the BMBF (grant 03SF0363B). One of the authors (Xianzhong Lin) gratefully acknowledges the financial support from the Chinese Scholarship Council, HZB and Helmholtz Association.

References

[1] K. Ito, T. Nakazawa, Jpn. J. Appl. Phys. 27 (1988) 2094.
[2] A. Ennaoui, M. Lux-Steiner, A. Weber, D. Abou-Ras, I. Kötschau, H.-W. Schock, R. Schurr, A. Hölzing, S. Jost, R. Hock, Thin Solid Films 517 (2009) 2511.
[3] D.A.R. Barkhouse, O. Gunawan, T. Gokmen, T.K. Todorov, D.B. Mitzi, Prog. Photovolt. Res. Appl. 20 (2012) 6.
[4] S. Bag, O. Gunawan, T. Gokmen, Y. Zhu, T.K. Todorov, D.B. Mitzi, Energy Environ. Sci. 5 (2012) 7060.
[5] R. Schurr, A. Hölzing, S. Jost, R. Hock, T. Voβ, J. Schulze, a. Kirbs, A. Ennaoui, M. Lux-Steiner, A. Weber, Thin Solid Films 517 (2009) 2465.
[6] S. Ahmed, K.B. Reuter, O. Gunawan, L. Guo, L.T. Romankiw, H. Deligianni, Adv. Energy Mater. 2 (2012) 253.
[7] B.A. Schubert, B. Marsen, S. Cinque, T. Unold, R. Klenk, S. Schorr, H.-W. Schock, Prog. Photovolt. Res. Appl. 19 (2011) 93.
[8] Q. Guo, G.M. Ford, W. Yang, B.C. Walker, E.A. Stach, H.W. Hillhouse, R. Agrawal, J. Am. Chem. Soc. 132 (2010) 17384.
[9] X.Z. Lin, J. Kavalakkatt, M. Lux-Steiner, A. Ennaoui, in: Proc. 26th Europ. Photovolt. Solar Energy Conf., Hamburg, 2011, p. 2896.
[10] P. Fernandes, P.M.P. Saloméa, A.F.D. Cunha, J. Alloys Compd. 509 (2011) 7600.
[11] D.B. Mitzi, O. Gunawan, T.K. Todorov, K. Wang, S. Guha, Sol. Energy Mater. Sol. Cells 95 (2011) 1421.
[12] N. Nakayama, K. Ito, Appl. Surf. Sci. 92 (1996) 171.
[13] F.Y. Shen, Wenxiu Que, X.T. Yin, Y.W. Huang, Q.Y. Jia, J. Alloys Compd. 509 (2011) 9105.
[14] X. Lin, A. Steigert, M. Lux-Steiner, A. Ennaoui, RSC Adv. 2 (2012) 9798.
[15] X. Fontané, L. Calvo-Barrio, V. Izquierdo-Roca, E. Saucedo, A. Pérez-Rodriguez, J.R. Morante, D.M. Berg, P.J. Dale, S. Siebentritt, Appl. Phys. Lett. 98 (2011) 181905.
[16] M. Altosaar, J. Raudoja, K. Timmo, M. Danilson, M. Grossberg, J. Krustok, E. Mellikov, Phys. Status Solidi A 205 (2008) 167.
[17] P.A. Fernandes, P.M.P. Salomé, F.D. Cunha, J. Phys. D 43 (2010) 215403.
[18] L.S. Price, I.P. Parkin, A.M.E. Hardy, R.J.H. Clark, Chem. Mater. 11 (1999) 1792.
[19] J.I. Pankove, Optical Processes in Semiconductors, Dover Inc., New York, 1975.
[20] K. Tanaka, Y. Fukui, N. Moritake, H. Uchiki, Sol. Energy Mater. Sol. Cells 95 (2011) 838.
[21] G.S. Babu, Y.B.K. Kumar, P.U. Bhaskar, V.S. Raja, Sol. Energy Mater. Sol. Cells 94 (2010) 221.
[22] T. Wada, S. Nakamura, Tsuyoshi Maeda, Prog. Photovolt. Res. Appl. 20 (2012) 520.
[23] J. Paier, R. Asahi, A. Nagoya, G. Kresse, Phys. Rev. B 79 (2009) 115126.
[24] A. Nagoya, R. Asahi, R. Wahl, G. Kresse, Phys. Rev. B 81 (2010) 113202.
[25] K. Tanaka, Y. Miyamoto, H. Uchiki, K. Nakazawa, H. Araki, Phys. Status Solidi A 203 (2006) 2891.
[26] Y. Miyamoto, K. Tanaka, M. Oonuki, N. Moritake, H. Uchiki, Jpn. J. Appl. Phys. 47 (2008) 596.

Please cite this article as: X. Lin, et al., Thin Solid Films (2012), http://dx.doi.org/10.1016/j.tsf.2012.10.034